Geometrical Design and Optimization of Stirrer for Friction Stir Welding

Nadhim M. Faleh*, Ridha A. Ahmed, Raad M. Fenjan

Al-Mustansiriah University, Engineering Collage
P.O. Box 46049, Bab-Muadum, Baghdad 10001, IRAQ

*Corresponding author's email: drnadhim [AT] gmail.com

ABSTRACT--- ***This paper investigates the influence of the pin geometry on mechanical properties of Aluminium 2024-T351 welded by friction stir welding (FSW). Square, triangle, and cylindrical pin geometries were studied for optimization due to the improvement ratio in tensile and bending strength. The results show that improvement ratio about 10% in mechanical properties was detected at the square pin case compared with the triangle and cylindrical pin geometries. The weld strength increases significantly by decreasing the feeding rate at all travel speeds. Calculations of the scanned zone by stirrer showed that the square pin produced the more significant mixing ratio compared to triangle pin. Development in mixing rate is about 15% by the square stirrer. Also, on the other hand, the results of the calculations of the scanned zone by stirrer pointing to that the size of mixing rate produced by the cylindrical pin is lower than the other types of tool.***

Keywords--- Friction, Stir, Welding, strength, stir-pin, Design, Mixing ratio, FSW, stirrer

1. INTRODUCTION

The rotational and travelling speeds as well as penetration depth are the main technological process parameters. The above technological parameters have an impact on forces acting on the FSP tool as well as the quality of modified surface. Thus, to obtain a defect free modified area, the parameters should be selected properly for any types of base material [1,2]. Furthermore, welding parameters such as tool rotation speed, traverse speed, and axial force have a significant effect on the amount of heat generation and strength of FSW joints. Macro structural evaluation showed the formation of tunnel defects due to inappropriate flow of plasticized metal [3]. In recent years, several papers have been published on various aspects of FSW. Moshwan et al. [4] comprehensively reviewed FSW tools and effect of tool rotational speed
on force generation, microstructure and mechanical properties of friction stir welded alloy. Azizieh et al. [5] gave a systematic review on effect of rotational speed and probe profile on microstructure and hardness of nanocomposites fabricated by friction stir processing. Golmohammadi et al. [6] and Alidokht et al. [7] and Huang et al. [8] comprehensively reviewed wear characterization of the surface metal matrix composite fabricated via friction stir processing. Dolatkhah et al. [9] and Zohoor et al. [10] investigated effects of process parameters on microstructural and mechanical properties.

The existing fusion welding techniques, most particularly resistance spot welding, cannot be used so effectively [11]. Many attempts have been tried while traditional fusion welding of Al and Mg alloys will produce coarse grains and massive brittle intermetallic compounds (IMCs) [11–18] . Aluminium (Al) alloys and lightweight materials of magnesium (Mg) are becoming more generally used due to the increasing demands for material recyclability and energy saving in the industry. In practical applications, Mg alloys are certainly faced up in joining Al alloys or steels[12–15]. The latter is considered to be harmful to the joint's mechanical properties [18,19].

The effectiveness of a Friction Stir Welding joint is robustly affected by various tool parameters: especially, geometrical parameters like the shape and the height of the pin; screwed, trapezoidal and cylindrical have a related influence on the heat generation and the metal flow due to friction forces [20-21]. Traverse speed, vertical pressure tool and the rotational speed of the device, on the plates during welding are the primary process parameters of Friction Stir Welding [22]. However, although, the tool geometry which involves the geometry of the Friction Stir Welding tool pin probe profile and tool shoulder is also an important characteristic which influences the weld strength. Therefore, the study of the Friction Stir Welding process also involves the study of tool characteristics and the investigation [23]. The Friction Stir Welding tool is a critical piece of this welding process. Thomas and Dawes [24] clarified in detail the tool development method took at outlined tool design and The Welding Institute aspects of the scroll shoulder idea. While there have been numerous studies concentrated on the difference of welding speeds and rotation to optimize the welding factors and study their microstructures for Al alloys, independent research has been approved out on the effects of tool structure [23]. FSW is being applied in many engineering uses, which desire the joining of dissimilar material collections, which are not applicable using traditional fusion welding methods. With the new developments in the technology of FSW, it is now

possible to perform different welding of Aluminium alloys, copper, magnesium, titanium and also other alloy combinations with several kinds of steels [25].

FSW is a welding process sophisticated later in 1991 using for Cu, Al, Ti, and Mg for work pieces, that could not be weld by traditional kinds of welding and lately develop excessive dissimilar enforcement because of quality consideration and economical. Modern kinds of tool advanced latterly for harder typed of materials work pieces as various kind of steels. Also diverse kinds of machines sophisticated for this aim. Friction Stir Welding can achieve by an ordinary CN machine for professional a single purpose robotic machine for small work pieces in orbital Friction Stir Welding-oil industries in steel pipes welding [26]. The schematic of friction stir process illustrated in Fig.1.

The process of FSW has been used in the automobile industries, shipbuilding, aerospace, and in many enforcement of commercial significance. That is because of several of its advantages over the traditional welding methods some of which involve very little spatter, porosity and distortion, no consumables, no fumes, no shielding gas requirements and no special surface treatment. Friction Stir Welding joints have made better mechanical properties which are free from blowholes or porosity related to traditionally welded materials. There are limited disadvantages in spite of those advantages, which also necessitate mentioning. Finally, the welding process leaves the exit hole after when the tool is exiting which is unwanted at the peak of the enforcement. This practice has been outdone, by providing compensation in the track for a continuous path, or by continuing into a plate for non-continual trajectories, or just by machining off the unwanted portion of the hole. Great down forces and static clamping of the plates to be welded are a requirement for this process which reasons restriction in the applicability, of this method to weld functions with convinced geometries [27]. In particular, the process may produce: fine grained structure, surface composite, microstructural modification of cast alloys, alloying with specific elements, improvement of welded joints quality [28].

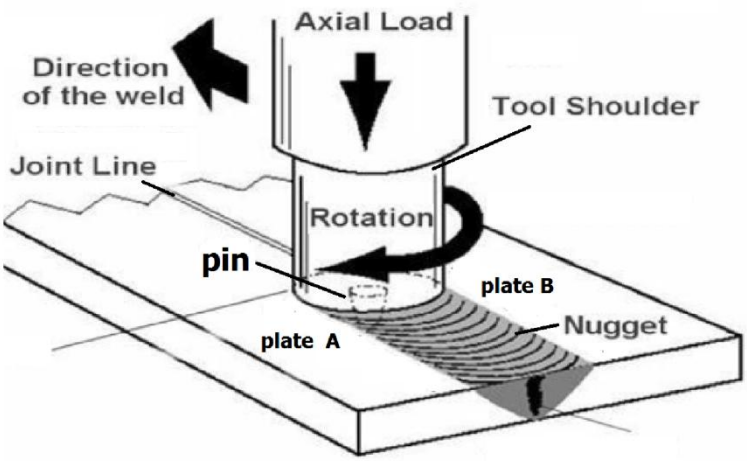

Figure (1). Friction stir welding operation

2. EXPERIMENTAL DETAILS

In this research, it was used Aluminium 2024-T351with data as shown in table 1 and 2. Friction stir welding operation was done by the pins with cylindrical, triangle and square geometry as shown in Figures 2. and 3. The base materials welded consisted of 6 mm thick. A controlled manual milling machine was utilized to fabricate Friction Stir Welding different joints, to produce welded plates as shown in figure 4. The specimens for bending and tensile tests were prepped due to detail in Figure 5.

Table (1): The standard and actual chemical composition of Aluminium 2024-T351.

Component Wt. %	Al	Cr	Cu	Fe	Mg	Mn	Si	Ti	Zn
Standard	90.7 94.7	Max 0.1	3.8 4.9	Max 0.5	1.2 1.8	0.3 0.9	Max 0.5	Max 0.15	Max 0.25
Actual	Bal.	0.08	4.1	0.28	1.43	0.56	0.33	0.08	0.16

Table (2): The standard and actual mechanical properties of Aluminium 2024-T351.

Mechanical Properties	Standard	Actual	Notes
Hardness, Brinell	120	126	AA; Typical; 500 g load; 10 mm ball
Hardness, Vickers	137	142	Converted from Brinell Hardness Value
Ultimate Tensile Strength	469 MPa	471 MPa	AA; Typical
Tensile Yield Strength	324 MPa	333 MPa	AA; Typical
Elongation at Break	19 %	18 %	AA; Typical; 1/2 in. (12.7 mm) Diameter
Modulus of Elasticity	73.1 GPa	74.1 GPa	AA; Typical; Average of tension and compression. Compression modulus is about 2% greater than the tensile modulus.
Poisson's Ratio	0.33	0.31	
Shear Modulus	28 GPa	29 GPa	
Shear Strength	283 MPa	288 MPa	AA; Typical

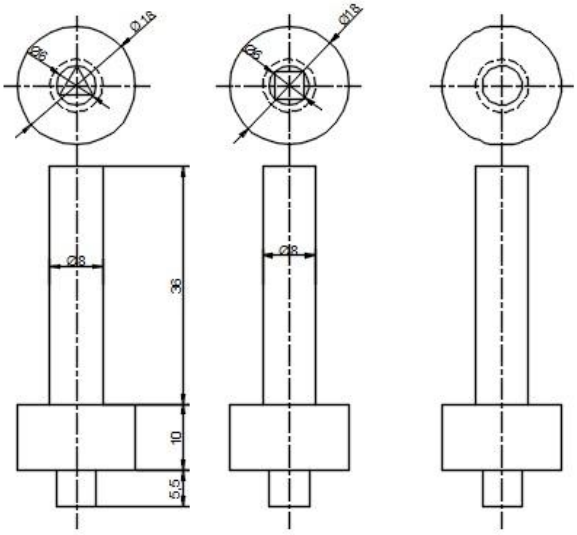

Figure (2). The FSW tools

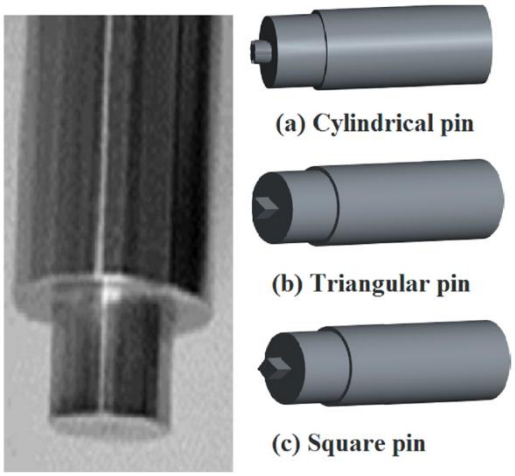

FIGURE 3The cylindrical, square and triangle geometry

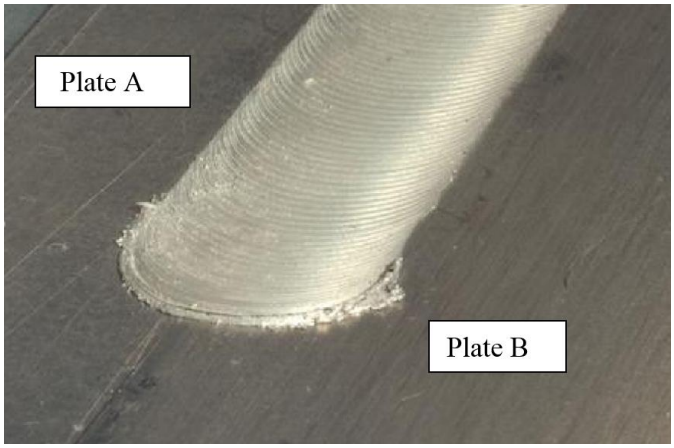

FIGURE 4 Welded specimens

The research was carried out in two stages: the first stage by using the same operating conditions, rotation speed of 500,750 and 1000rev/min with a constant feed rate of 30mm/min for comparison among the three shapes of the pin. But in the second stage, several operating conditions were used, the rotations of the tool, with various values of feeding rates shown in table 3, to determine the effect of the speed of machine on the effectiveness of the geometry of the pin.

Table (3): The operating conditions of FSW.

Operating condition	1st stage	2nd stage		
		Case1	Case2	Case3
Tool speed (rpm)	500,750,1000	500	750	1000
Feed rate (mm/min)	30	15,30,45	15,30,45	15,30,45

Tensile and bending samples were manufactured after the FSW welding process was performed due to specimens as shown in the figure 5. The tensile test according to ASTM-B557M and the standard bending test according to ASME QW-462.

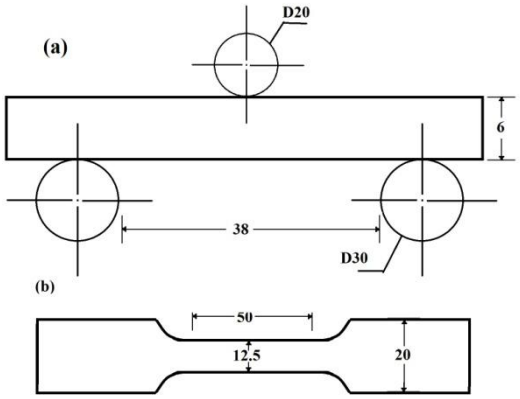

FIGURE 5 The specimens (a) bending (b) tensile.

3. EXPERIMENTAL RESULTS

All the results of preliminary work; mechanical properties for cases of the square, triangle, and cylindrical pins geometries were mentioned in the Tables 4-7. The Tensile strength, ultimate tensile strength and elongation of welded specimens were compared with the base material in Table 4. The welded specimens were produced by the first stage with a contant operating conditions; 500rpm and 30mm/min.

Table (4): The mechanical properties of FSW in 1st step.

Stirrer Type (operating condition; 500 r.p.m, 30mm/min)	**Base material**			**Welded Joint**			
	Tensile strength	**Ultimate tensile strength**	**Elongation**	**Tensile strength**	**Ultimate tensile strength**	**Elongation**	**Bending load**
	[Mpa]	**Rm [Mpa]**	**A [%]**	**[Mpa]**	**Rm [Mpa]**	**A [%]**	**KN**
Cylindrical	333	471	18	242	336	11.0	11.2
triangle				269	352	9.1	11.3
Square				290	409	8.0	12.4

Also, the tensile strength, ultimate tensile strength, bending load and elongation for welded specimen by the cylindrical pin geometry were compared due to different speeds and feeding rates mentioned in speeds and feeding rates were pointed out in Table 5.

Table (5): The mechanical properties of FSW in 2nd step for cylindrical pin.

Rotational speed;	**Feed** mm/min	**Welded Joint**			
		Tensile strength $R_{p0.2}$ [Mpa]	**Ultimate tensile strength Rm [Mpa]**	**Enlongation A [%]**	**Bending load KN**
500	15	249	347	10.1	11.5
	30	242	336	11.0	11.2
	45	237	332	11.3	10.7
750	15	236	339	9.6	10.6
	30	223	331	10.2	10.0
	45	212	324	10.5	9.7
1000	15	230	332	11.9	10.0
	30	220	326	12.1	9.5
	45	206	320	12.4	8.7

The tensile strength, ultimate tensile strength, bending load and elongation for welded specimen by the triangular pin geometry were compared due to different speeds and feeding rates mentioned in speeds and feeding rates were pointed out in Table 6.

Table (6): The mechanical properties of FSW in 2nd step for triangle pin.

Rotational speed;	**Feed** mm/min	**Welded Joint**			
		Tensile strength $R_{p0.2}$ [Mpa]	**Ultimate tensile strength Rm [Mpa]**	**Enlongation A [%]**	**Bending load KN**
500	15	278	376	8.9	11.7
	30	269	352	9.1	11.3
	45	259	348	9.5	10.8
750	15	268	369	8.7	11.1
	30	259	361	9.2	10.5
	45	251	353	10.0	9.8
1000	15	259	359	8.9	10.9
	30	253	353	9.5	10.3
	45	247	348	10.4	9.5

The tensile strength, ultimate tensile strength, bending load and elongation for welded specimen by the square pin geometry were compared due to different speeds and feeding rates mentioned in speeds and feeding rates were pointed out in Table 7.

Table (7): The mechanical properties of FSW in 2nd step for Square pin.

Rotational speed;	**Feed** mm/min	**Welded Joint**			
		Tensile strength $R_{p0.2}$ [Mpa]	**Ultimate tensile strength Rm [Mpa]**	**Enlongation A [%]**	**Bending load KN**
500	15	298	411	7.8	12.8
	30	290	409	8.0	12.4
	45	279	402	8.3	11.9
750	15	288	399	8.1	12.0
	30	279	391	8.6	11.6
	45	268	383	9.0	10.9
1000	15	279	389	8.4	11.1
	30	269	383	8.7	10.7
	45	263	378	9.4	9.9

The charts due to the experimental results of this research; mechanical properties for cases of Square, triangle, and cylindrical pins geometries were mentioned in the Figures 6-9.The tensile strength, ultimate tensile strength, elongation and bending load were compared due to different geometries at a speed of 500,750 and 1000rpm with feeding rate of 30mm/min.

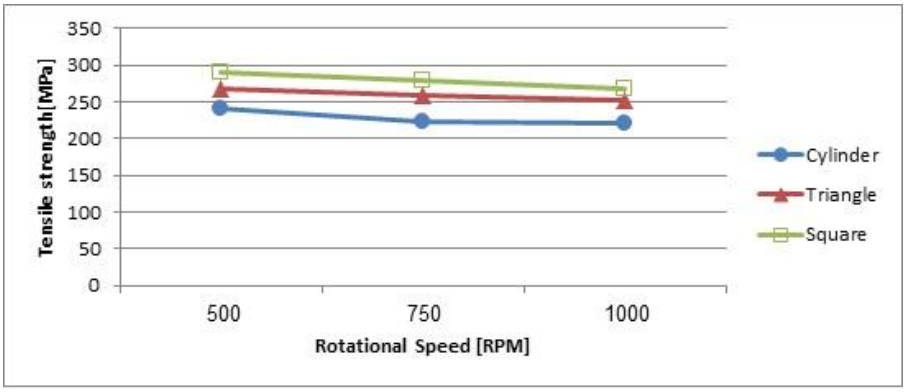

Figure 6 The tensile stress versus RPM and tool shape.

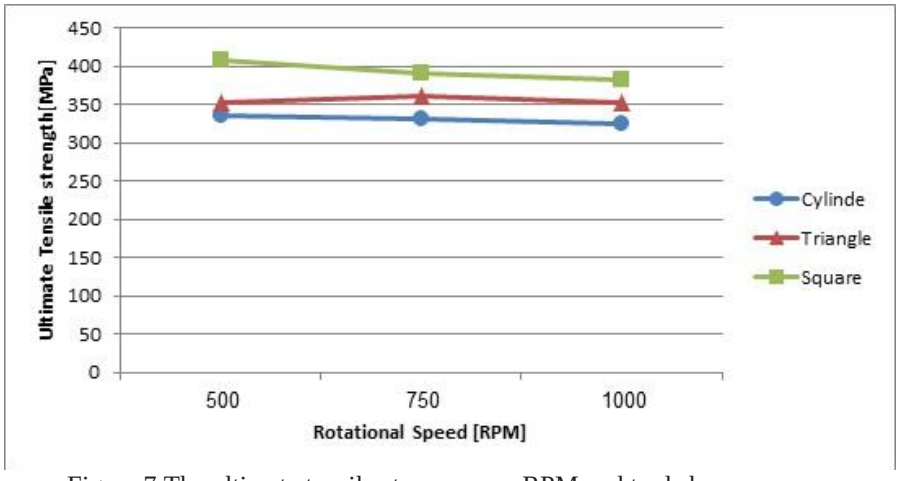

Figure 7 The ultimate tensile stress versus RPM and tool shape.

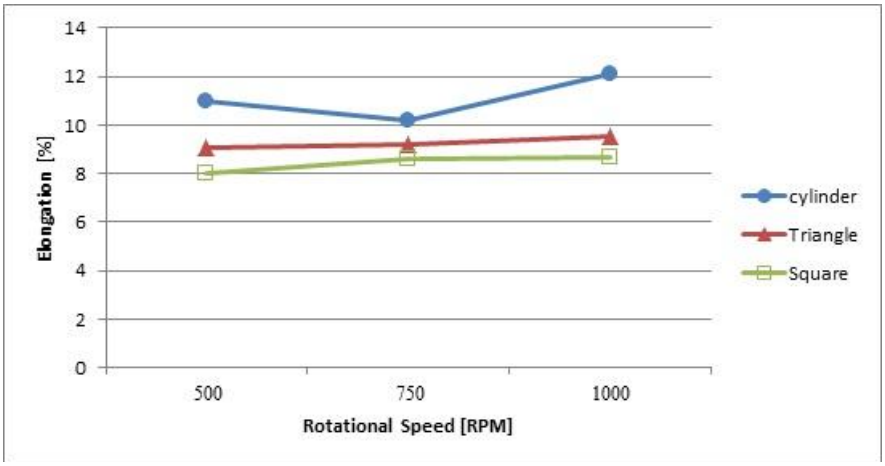

Figure 8 The elongation versus RPM and tool shape.

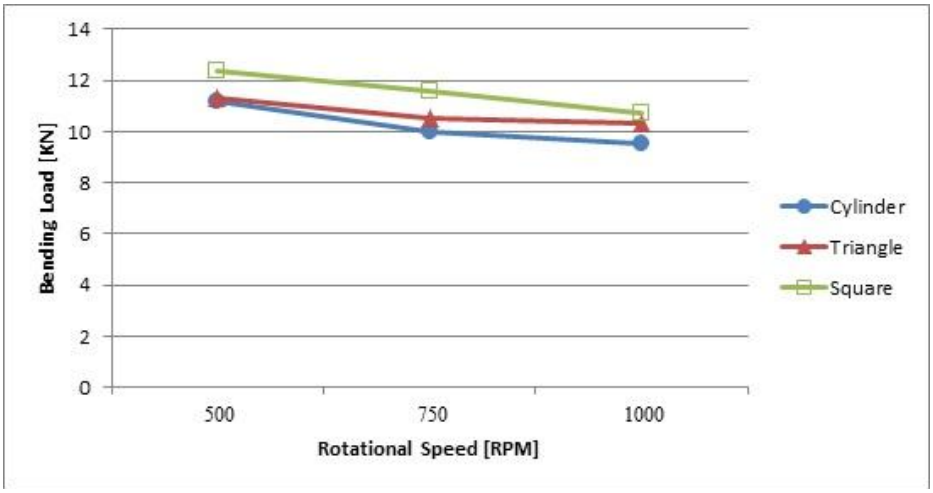

Figure 9 The bending load versus RPM and tool shape.

Also, the tensile strength, ultimate tensile strength, elongation and bending load for welded specimen by the cylindrical pin geometry were compared due to different speeds and feeding rates were mentioned in the Figures10-13. The tensile strength, ultimate tensile strength, elongation and bending load for welded specimen by the triangular pin geometry were compared due to different speeds and feeding rates were mentioned in the Figures 14-17. The tensile strength, ultimate tensile strength, elongation and bending load of the welded specimen by the rectangular pin geometry were compared due to different speeds and feeding rates were mentioned in the Figures 18-21.

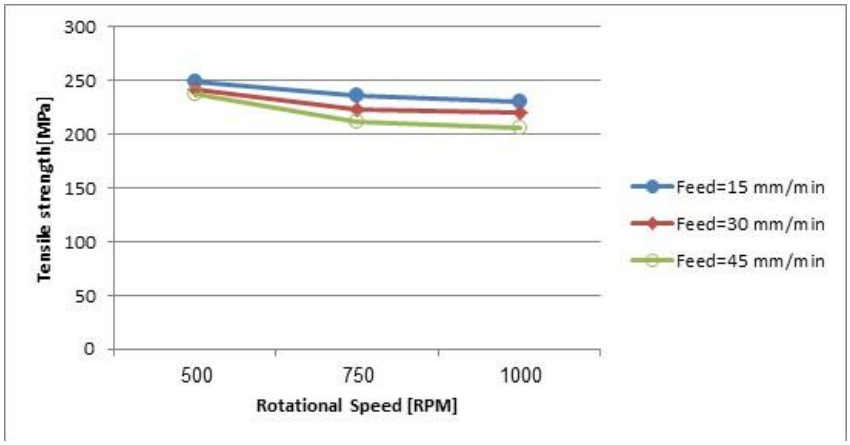

Figure 10 The tensile stress versus RPM for cylindrical pin

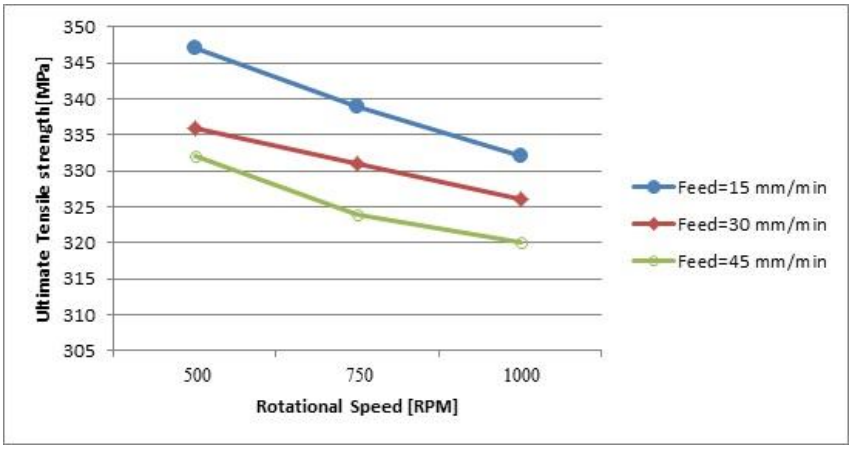

Figure 11 The ultimate tensile stress versus RPM for cylindrical pin

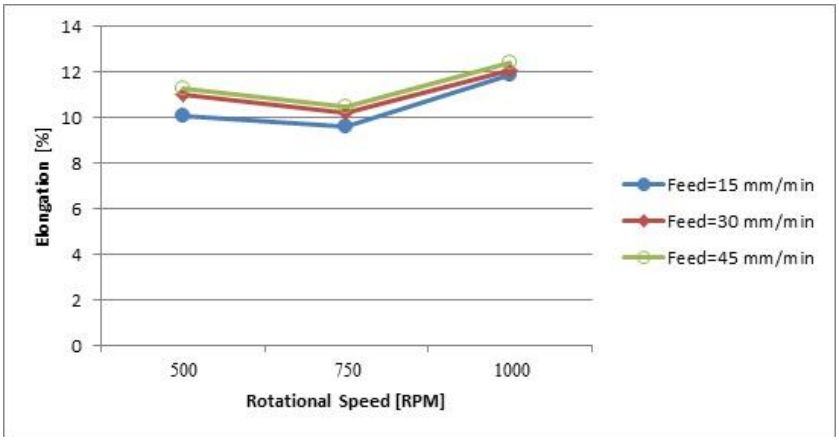

Figure 12 The elongation versus RPM for cylindrical pin

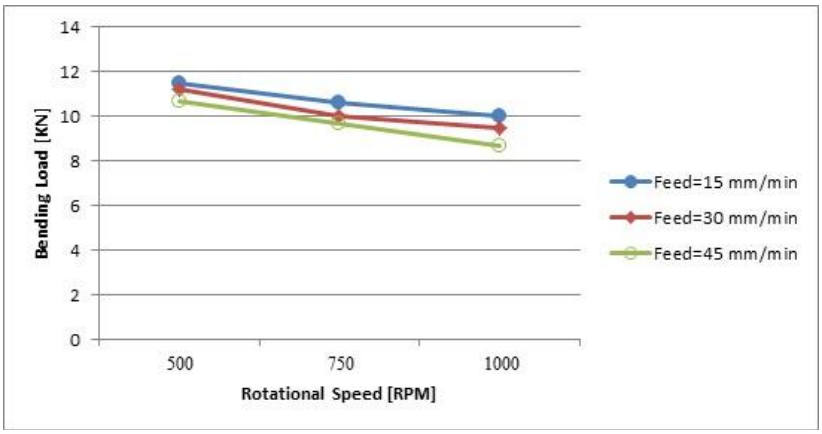

Figure 13 The bending load versus RPM for cylindrical pin.

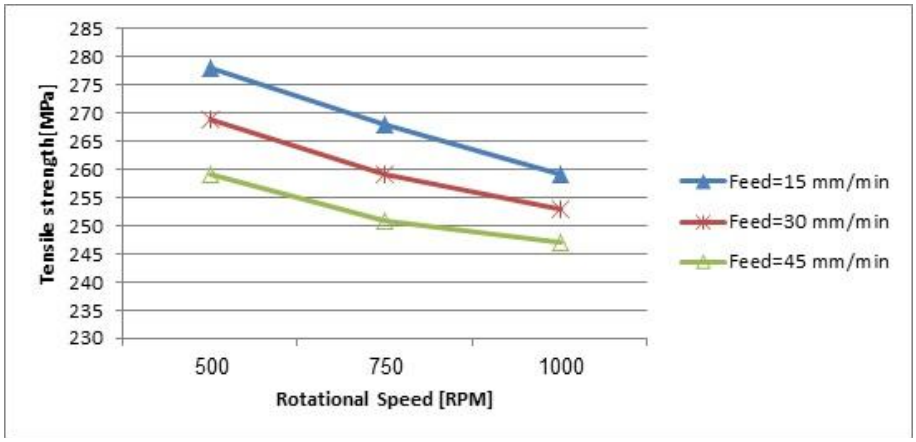

Figure 14 The tensile stress versus RPM for triangle pin.

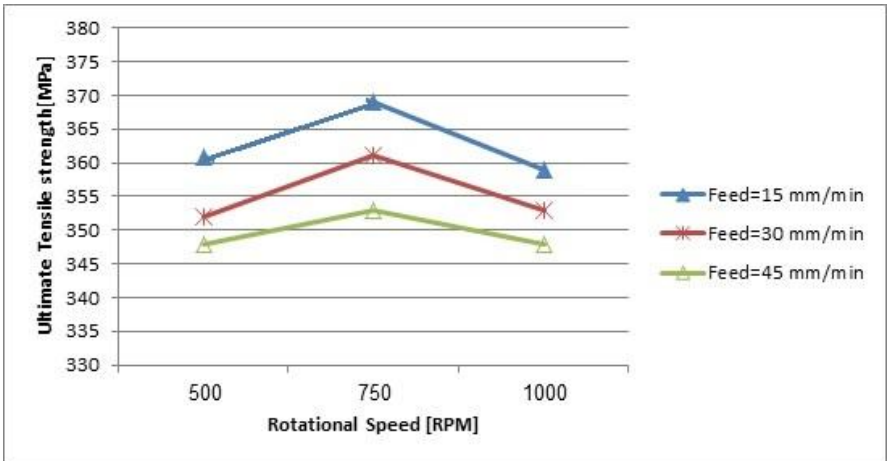

Figure 15 The ultimate tensile stress versus RPM for triangle pin.

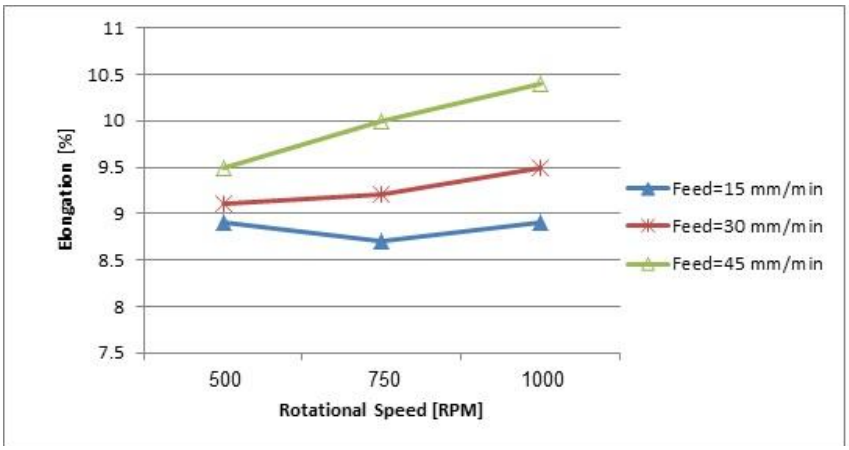

Figure 16 The elongation versus RPM for triangle pin.

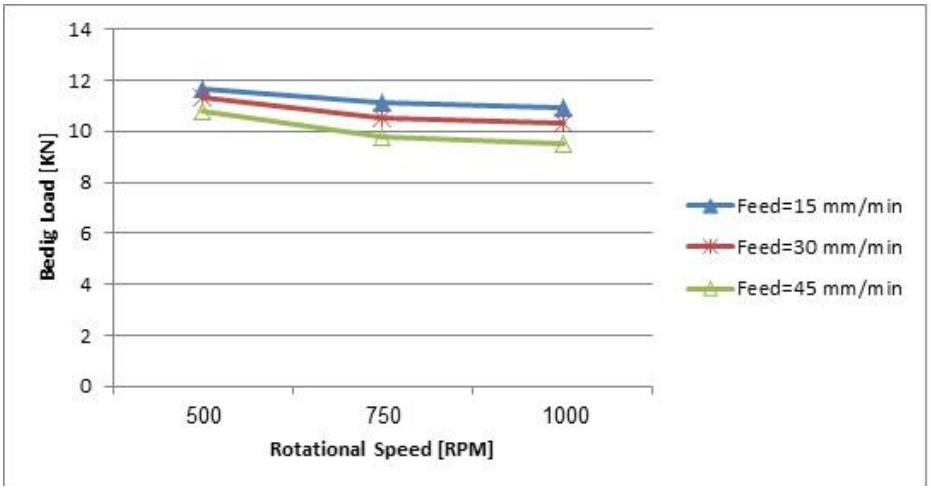

Figure 17 The bending load versus RPM for triangle pin.

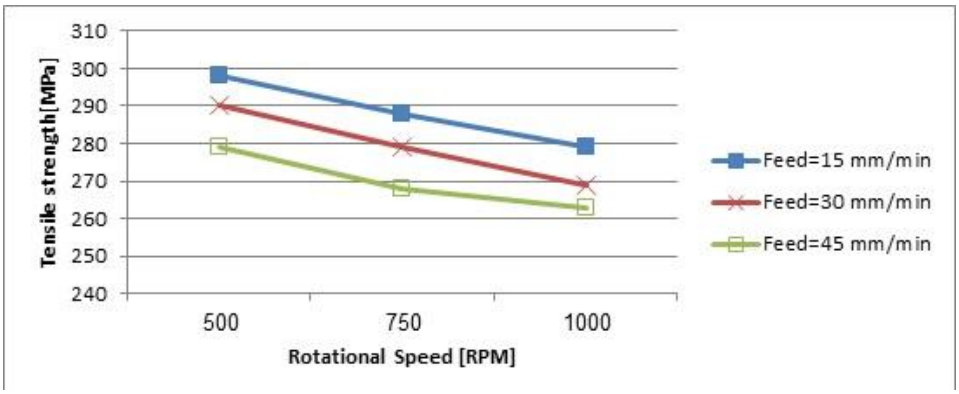

Figure 18 The tensile stress versus RPM for square pin

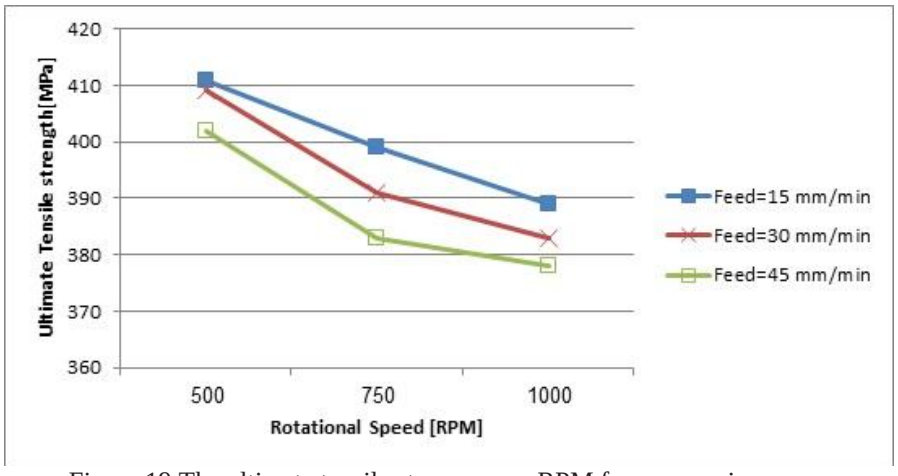

Figure 19 The ultimate tensile stress versus RPM for square pin

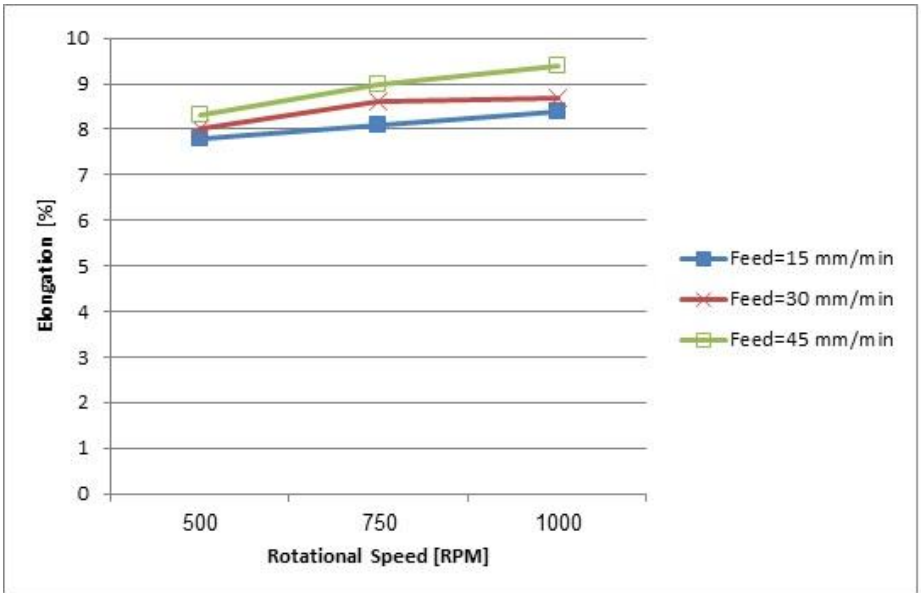

Figure 20 The elongation versus RPM for square pin

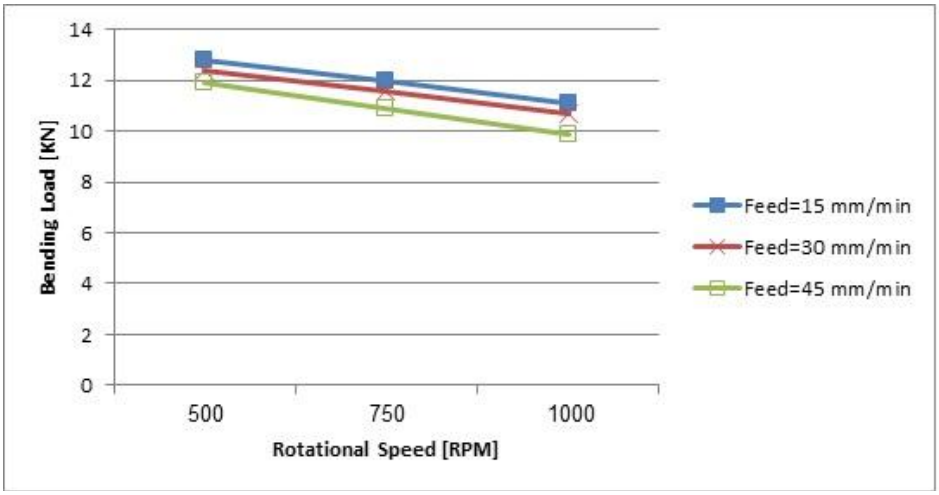

Figure 21 The bending load versus RPM for square pin

4. ANALYSIS OF THE RESULTS

The comparison between the pins with square and triangle geometry was based on the assumption of the tools shown in Fig.2. Calculations for the scanned zone by pin (tool) grounded on the assumption that the centre of the square to be the origin. The entire function decreases the working Cartesian plane to just the first quadrant.

The maximum function confirms that either the x-value or y-value is equal to c. If the absolute capacity is not an exploit, then (-c <x< c). So, y must be either -c or c. Therefore, there are two horizontal parallel lines, similarly, vice versa, creating two vertical parallel lines.

Max (abs(x), abs(y)) = c (1)

The square-shaped by the max (abs) way has a width of 2c. The square-shaped by the L1 norm way has a width of Sqrt (2)*c. As shown in Fig. 22, so: $(r.sin\theta)^2 + (r.cos\theta)^2 = r^2$ (2)

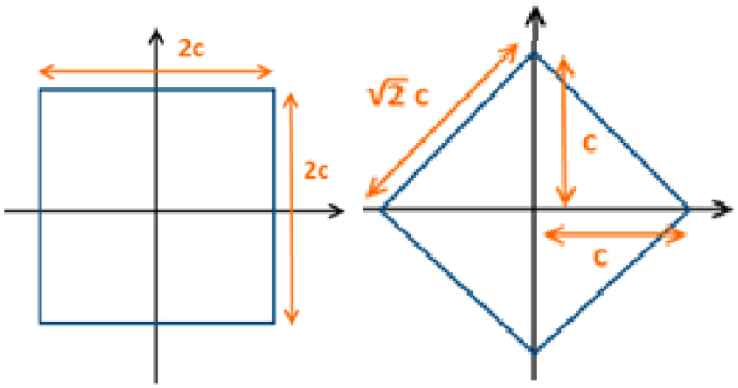

Figure (22).The rotation of stirrer

Fig.23 shows the nature of the path resulting from the movement of the stirrer and its rotation. As well as the area of the pin scans during rotation. Fig. 24 shows the relationship between feed and the scanned area, where the field increases with increasing of feed.

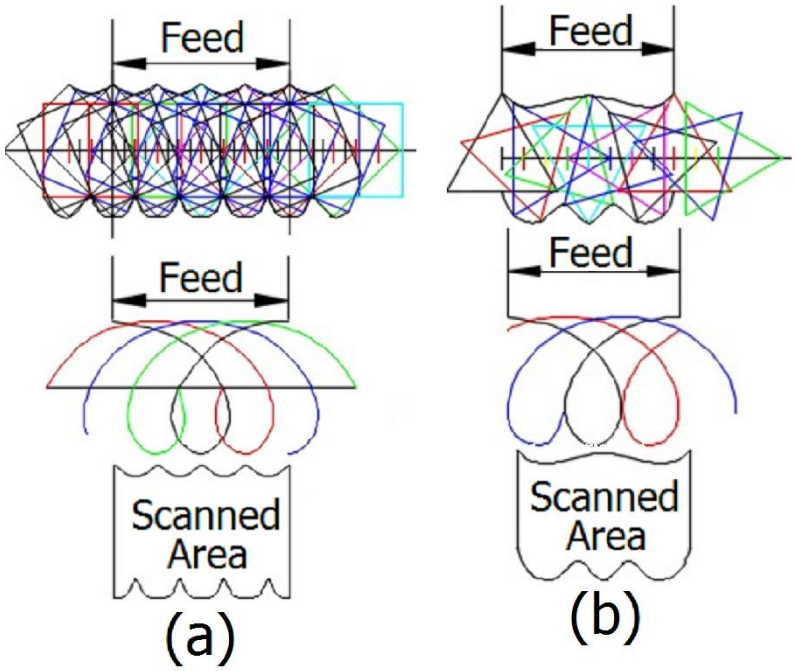

Figure (23).The scanned areas (a) square (b) triangle

The excerpts of operating conditions were based on the research of G. Elatharasan[28], which looks at the preliminary examination and optimization of process parameters on Friction Stir Welding of Al Alloy. Also in the study of M. Ghosh [19] which focuses on optimization of FSW parameters for Al alloys, the parameters of operation were excerpted due to the reviews of many researchers [30-34].

Comparison between the circular motion of the square shape and the circular motion of the triangle shape: Figure 24 shows the shape of a square and another triangle placed within a radius (R), each of which has a circular motion within the circle at an angle of (Θ), as shown in Figure 25. The circular section formed by this angle is equal to each of them. As a result of the geometric disintegration, we have another small sector shown in Figure (26). The area of this sector is different for both forms.

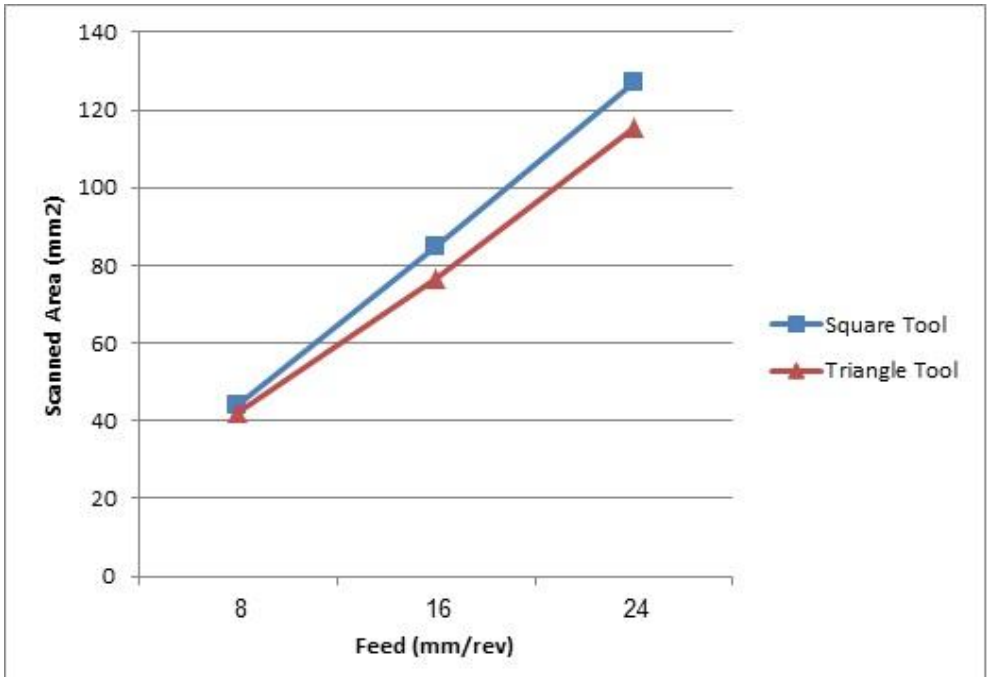

Figure (22).The relation between feed and scanned area

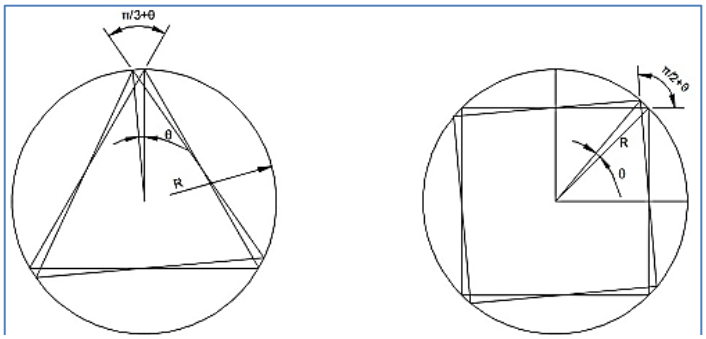

Figure 25 The motion within an angle of (Θ)

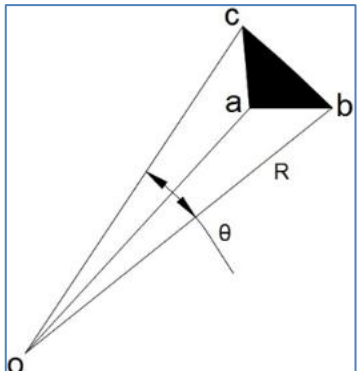

Figure 23 The area of this sector is different for both forms.

From fig.(2), using sine law:

$$\frac{R}{\sin a} = \frac{l}{\sin \frac{\theta}{2}}$$

$$l = \frac{R.\sin \frac{\theta}{2}}{\sin a}$$

For square shape:

$$a = \frac{3\pi - 2\theta}{4}$$

$$l = \frac{R.sin\frac{\theta}{2}}{\sin\frac{3\pi-2\theta}{4}}$$

Area (A) of sector (abo) $A_{abo} = \frac{1}{2}.l.R.\sin\frac{\pi}{4}$

$$= \frac{1}{2\sqrt{2}}.l.R$$

Total area of sector (obc) $A_T = \frac{\pi.R^2.\theta}{360}$

$A_{abc} = A_T - 2A_{abo}$

$$A_{abc} = \frac{\pi.R^2.\theta}{360} - \frac{l.R}{\sqrt{2}} \qquad (1)$$

For triangle shape:

$$a = \frac{5\pi - 3\theta}{6}$$

$$l = \frac{R.sin\frac{\theta}{2}}{\sin\frac{5\pi-3\theta}{6}}$$

Area (A) of sector (abo) $A_{abo} = \frac{1}{2}.l.R.\sin\frac{\pi}{6}$

$$= \frac{1}{4}.l.R$$

$$A_{abc} = \frac{\pi.R^2.\theta}{360} - \frac{l.R}{2} \qquad (2)$$

It can be concluded that the area of the formed area of the triangle is larger than the square shape as shown in figure 24. This means that the square shape is a circle during its rotational motion and it is greater than the circle which is achieved by the triangular shape. The box is larger than the triangle shape.

5. CONCLUSION

The movement of the tool with a particular feed (f) and a rotation with N speed, results in the transfer of the material from plate A to plate B, which causes a mixing between the metal of plates. The time of blending depends on the following factors; First: the pin geometry. Second: operating conditions; feed mm/rev and tool rotation. Calculations of the scanned zone by stirrer show that the square pin produces the more significant mixing ratio compared to triangle pin. Development in mixing rate is about 15% by the square stirrer. Also, on the other hand, results of the calculations of the scanned zone by stirrer specified that the size of mixing rate fulfil by the cylindrical pin is smaller than the different types of tools and approached to zero.

6. REFERENCES

[1] N. Mendes, P. Neto, A. Loureiro, et al., Machines and control systems for friction stir welding: a review, Materials and Design 910 (2016) 256–265.
[2] C. Hamilton, M.St. Węglowski, S. Dymek, P. Sedek, Using a coupled thermal/material flow model to predict residual stress in friction stir processed AlMg9Si, Journal of Materials Engineering and Performance 24 (2015) 1305–1312.
[3] Omar S. Salih, Hengan Ou. W. Sun, D. G. McCartney, A review of friction stir welding of aluminium matrix composites, Materials and Design 86 (2015) 61–71.
[4] R. Moshwan, F. Yusof, et al., Effect of tool rotational speed on force generation, microstructure and mechanical properties of friction stir welded Al–Mg–Cr–Mn (AA 5052-O)
alloy, Materials and Design 66 (2015) 118–128.

[5] M. Azizieh, A.H. Kokabi, P. Abachi, Effect of rotational speed and probe profile on microstructure and hardness of AZ31/ Al2O3 nanocomposites fabricated by friction stir processing, Materials and Design 32 (2011) 2034–2041.
[6] M. Golmohammadi, M. Atapour, A. Ashrafi, Fabrication and wear characterization of an A413/Ni surface metal matrix composite fabricated via friction stir processing, Materials and Design 85 (2015) 471–482.
[7] S.A. Alidokht, A. Abdollah-zadeh, et al., Microstructure and tribological performance of an aluminium alloy based hybrid composite produced by friction stir processing, Materials and Design 32 (2011) 2727–2733.
[8] Y. Huang, Y. Wang, et al., Microstructure and surface mechanical property of AZ31 Mg/SiCp surface composite fabricated by direct friction stir processing, Materials and Design 59 (2014) 274–278.
[9] A. Dolatkhah, P. Golbabaei, et al., Investigating effects of process parameters on microstructural and mechanical properties of Al5052/SiC metal matrix composite fabricated via friction stir processing, Materials and Design 37 (2012) 458–464.
[10] M. Zohoor, M.K.B. Givi, P. Salami, Effect of processing parameters on fabrication of Al-Mg/Cu composites via friction stir processing, Materials and Design 39 (2012) 358–365.
[11] H.M. Rao, J.B. Jordon, B. Ghaffari, X. Su, A.K. Khosrovaneh, M.E.
[12] H. Rao, B. Ghaffari, W. Yuan, J. Jordon, H. Badarinarayan, Mater. Sci. Eng. A 651 (2016) 27–36. Barkey, et al., Int. J. Fatigue 82 (2016) 737–747.
[13] B. Ratna Sunil, G. Pradeep Kumar Reddy, A.S.N. Mounika, P. Navya Sree, P. Rama Pinneswari, I. Ambica, et al., J. Magnes. Alloys 3 (2015) 330–334.
[14] J.P. Bergmann, R. Schuerer, K. Ritter, Key Eng. Mater. 549 (2013) 492–499.
[15] U. Singarapu, K. Adepu, S.R. Arumalle, J. Magnes. Alloys 3 (2015) 335–344.
[16] A. Ben-Artzy, A. Munitz, G. Kohn, B. Bronfin, A. Shtechman, Magnes. Tech. (2002) 295–302.
[17] L. Liu, H. Wang, G. Song, J.N. Ye, J. Mater. Sci. 42 (2007) 565–572. [8] N. Yamamoto, J. Liao, S. Watanabe, K. Nakata, Mater. Trans. 50 (2009) 2833–2838.
[18] Marek Stanisław Węglowski, Friction stir processing – State of the art, Archives of Civil and Mechanical Engineering 18 (2 0 1 8) 114–129. [19] Y. Chen, K. Nakata, Scr. Mater. 58 (2008) 433–436.
[20] Rai, R., De, A., Bhadeshia, H., DebRoy, T., (2011) "Friction stir welding tools." Science and Technology of Welding and Joining, 16, 325-342.
[21] Zhang, Y., Cao, X., Larose, S., Wanjara, P., (2012) "Review of tools for friction stir welding and processing." Canadian Metallurgical Quarterly 51, 250-261.
[22] Rajakumar, S., Muralidharan, C., Balasubramanian, V., (2010)"Optimization of the friction stir welding process and tool parameters to attain a maximum tensile strength of AA7075–T6 aluminum alloy". Journal of Engineering Manufacture 224, 1175-1191.
[23] Leal, R., Leitao, C., Loureiro, A., Rodrigues, D., Vilaça, P., (2008)"Material flows in heterogeneous friction stir welding of thin al sheets: effect of shoulder geometry." Materials Science and Engineering: A 498, 384-391.
[24] Dawes, C., Thomas, W., 1999, "Development of Improved Tool Designs for FSW of Aluminum." Proceedings of the First International Conference on Friction Stir Welding, 2-6.
[25] T. DebRoy and H. Bhadeshia, Sci-Technol Weld Joining, (2010), 15(4), 266-270.
[26] N. T. Kumbhar and K. Bhanumurthy, (2008) "Friction Stir Welding of Al 6061 Alloy Materials", Science Division Bhabha Atomic Research Centre Trombay, Mumbai – 400085, India Asian J. Exp. Sci., Vol. 22, No. 2,; pp. 63-74.
[27] P. Murali Krishna, N. Ramanaiah and K. PrasadaRao, (2013) "optimization of process parameters for Friction Stir Welding of Dissimilar Aluminium alloys (AA2024-T6 and AA6351-T6) by using Taguchi Method", International Journal of Industrial Engineering Computations 4 pp. 71-80.
[28] G. Elatharasan and V. S. Senthil Kumar, (2013), "An Experimental Analysis and Optimization of process parameters on Friction Stir Welding of AA 6061 – T6 Al Alloy using RSM," International Conference on Design and Manufacturing, IConDM, pp. 1227-1234.
[29] M. Ghosh, K. Kumar, S.V. Kailas, A. K. Ray, (2010) "Optimization of Friction Stir Welding parameters for dissimilar Al Alloys" Material and Design, 31, pp. 3033-3037.
[30] Pouranvari, M., (2011) "TLP Bonding of A Gamma Prime Strengthened Super alloy Using Ni-Si-B Interlayer at 1150°C Part II: Mechanical Properties", World Applied Sciences Journal, 15(11), pp. 1532-1533.
[31] Kumar R., M. Siva Pragash, and S. Varghese, (2013) "Optimizing the Process Parameters of FSW on AZ31BMg Alloy by Taguchi-Grey Method", Middle East Journal of Scientific Research, 15 (1), pp. 161-167.
[32] Mustafa Boz, Adem Kurt, (2004), "The Influence of Stirrer Geometry on Bonding and Mechanical Properties in friction stir welding process," Journal of Materials and Design, Volume 25, pp. 343-347.
[33] SriramulaSai Kumar, P. Satish Kumar, (2015), "Characterization and Processing of Friction Stir Welding on Copper Welds"International Journal of Research in Engineering and Technology, Volume: 04, Issue: 11.
[34] A. Pradeep, S. Muthukumaran, (2013), "An Analysis to Optimize The Process Parameters of FSW Low Alloy Steel Plates," International Journal of Engineering, Science, and Technology, Vol. 5, No. 3, pp. 25-35.